Bromate Removal from Water Using Ion Exchange Resin: Batch and Fixed Bed Column Performance

Safal Mestri, Sedar Dogan & Chedly Tizaoui

Published online: 29 Aug 2022.

Submit your article to this journal

View related articles

View Crossmark data

Taylor & Francis
Taylor & Francis Group

Bromate Removal from Water Using Ion Exchange Resin: Batch and Fixed Bed Column Performance

Safal Mestri, Sedar Dogan, and Chedly Tizaoui

Water and Resources Recovery Research Lab, Department of Chemical Engineering, Faculty of Science and Engineering, Swansea University, Swansea, SA1 8EN, UK

ABSTRACT

In this study, the removal of bromate, a regulated ozone by-product, was evaluated using a strong-base anion (SBA) exchange resin in batch and column experiments. The kinetics studies in batch mode showed that film diffusion-controlled bromate exchange in SBA and the isotherm studies showed that the Langmuir model fitted the experimental results with a maximum exchange capacity of 296.66 mg BrO_3^-/g (~1.3 meq/mL resin). In the fixed-bed column studies, breakthrough curves were obtained under different operating conditions to examine the effects of feed flow rate, inlet bromate concentration, and bed height on column performance. A modified n-order Bohart and Adams model (n-BAM-c), which considered the asymmetry of the breakthrough curve and flow channeling, was applied for the first time to describe the experimental data obtained from the column and to predict the breakthrough curves. It was found that n-BAM-c fitted the experimental data well ($R^2 > 0.99$) and the effects of the key operating conditions on the model parameters were determined. Overall, the results show that SBA exchange is suitable for bromate removal from water and n-BAM-c could be a powerful tool for the design and upscaling of bromate ion exchange columns.

Introduction

Various chemical disinfection and oxidation processes are employed in water purification and wastewater treatment such as ozonation and chlorination to degrade contaminants and inactivate microorganisms (Collivignarelli, Abbà, Benigna, Sorlini, Torretta 2018). However, since water sources are complex matrices and contain many ions and compounds, intensive disinfection and oxidation can lead to the formation of several unwanted organic and inorganic by-products, known as disinfection by-products (DBP) (Collivignarelli, Abbà, Benigna, Sorlini, Torretta 2018). Some of these by-products are harmful to human health and the environment. Particularly, bromate (BrO_3^-) has been the stimulus for more research because it is reported as a potential human carcinogen by the International Agency for Research on Cancer (IARC) (WHO 2005). The occurrence of bromate in water is primarily due to the ozonation of waters containing bromide (Br^-) ions through complex reactions involving molecular ozone and hydroxyl radicals (New York State Department of Health 2017). Ozone is an excellent oxidant and disinfectant which is widely used in the water industry as it can destroy or

deactivate microorganisms (e.g., protozoa and cryptosporidium oocysts), improve the taste and odor of water, and remove micropollutants from water and wastewater (Tizaoui and Zhang, 2010; Tizaoui, Grima, Hilal 2011; Mansouri, Tizaoui, Geissen, Bousselmi 2019). Bromide ions are present in surface water mainly due to salt water intrusion and these ions can form significant amounts of bromate upon reaction with ozone (VanBriesen n.d.). Bromate formation in drinking water is affected by several factors such as Br^- ion concentration, ozone dosage, reaction time, temperature, and pH of the source water (Tynan, Lunt, Hutchison 1993; Yang, Dong, Jiang, Wang, Liu 2019a). The pathways for bromate formation via ozonation involves the intermediary hypobromite ion (OBr^-) as described by reactions 1–3 below (Yang, Dong, Jiang, Wang, Liu 2019a):

$$O_3 + Br^- \longleftrightarrow {}^-OOOBr \to BrO^- + O_2, k_1$$
$$= 160 - 258 \ M^{-1}s^{-1} \quad [1]$$

$$O_3 + BrO^- \to BrO_2^- + O_2, k_2 = 100 \ M^{-1}s^{-1} \quad [2]$$

$$O_3 + BrO^- \to Br^- + 2O_2, k_3 = 330 \ M^{-1}s^{-1} \quad [3]$$
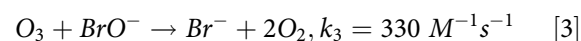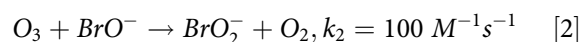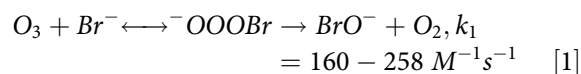
CONTACT Chedly Tizaoui ✉ C.Tizaoui@Swansea.ac.uk 🖥 Water and Resources Recovery Research Lab, Department of Chemical Engineering, Faculty of Science and Engineering, Swansea University, Swansea, SA1 8EN, UK

$$O_3 + BrO_2^- \rightarrow BrO_2 + O_3^-, k_4 = 8.9 10^4 \ M^{-1}s^{-1} \quad [4]$$
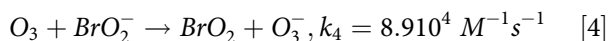
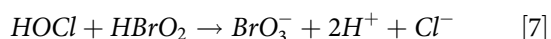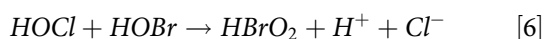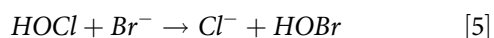Besides ozonation, bromate can be formed in advanced oxidation processes when hydrogen peroxide coupled with O_3 and in ferrate (VI) oxidation (Arvai, Jasim, Biswas 2012; Huang et al. 2016). Bromate was also detected in water after other advanced treatment methods such as ultraviolet combined treatments with chlorine (UV/chlorine), with persulfate (UV/persulfate) and cupric oxide (CuO) chlorination (Huang, Gao, Deng 2008; Fang and Shang, 2012; Liu, von Gunten, Croué 2012). During chlorination, chlorine, in the form of hypochlorous acid (HOCl), oxidizes Br^- to hypobromous acid (HOBr), which is further oxidized to bromous acid ($HBrO_2$) to finally produce bromate, as shown in following reactions 5–7 (Tynan, Lunt, Hutchison 1993).

$$HOCl + Br^- \rightarrow Cl^- + HOBr \quad [5]$$

$$HOCl + HOBr \rightarrow HBrO_2 + H^+ + Cl^- \quad [6]$$

$$HOCl + HBrO_2 \rightarrow BrO_3^- + 2H^+ + Cl^- \quad [7]$$

Bromate formation during chlorination was enhanced in the presence of CuO. Moreover, the possibility of bromate formation in advanced oxidation processes of Br^- containing water such as H_2O_2/O_3 has been proposed (Tynan, Lunt, Hutchison 1993). The reaction mechanism is shown below.

$$H_2O_2 + BrO^- \rightarrow BrO_2^- + H_2O \quad [8]$$

$$BrO_2^- + BrO^- \rightarrow BrO_3^- + Br^- \quad [9]$$
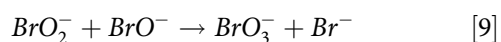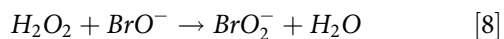
Several health effects have been reported on ingestion of large amounts of bromate such as nausea, vomiting, abdominal pain, diarrhea, as well as effects on the kidney and nervous system (New York State Department of Health 2017). Some effects are reported as irreversible such as hearing loss and renal failure (WHO 2005). Bromate has also been proved to induce follicular cell tumors of thyroid and renal cell tumors which led to categorizing bromate as a potential carcinogen under certain dose conditions by the United States Environmental Protection Agency (US EPA). One significant research has also suggested that bromate induces oxidative stress from intracellular within kidney cells leading to DNA damage (WHO 2005) and chronic exposures to bromate cause testicular mesothelial and thyroid tumors in rats (Delker et al. 2006). Based on the assumptions about human cancer risks and toxic effects, EPA and World Health Organization (WHO) have promulgated a bromate concentration level of 10 μg/L in drinking water (WHO 2005; Yang, Dong, Jiang, Wang, Liu 2019a). The same bromate concentration limit was proposed by the European Commission and China (Delker et al. 2006; JRC 2016).

Several techniques have been developed to reduce bromate concentration in drinking water. The primary techniques were based on lowering the possibility for bromate formation such as lowering bromide concentration in raw water before ozonation, controlling ozone reaction time, lowering water pH, and converting bromate back to bromide by catalytic hydrogenation using hydrogen gas (WHO 2005; Yang, Dong, Jiang, Wang, Liu 2019a). A review states that there is a threshold of bromide concentration (0.18–0.3 mgL^{-1}), below which bromate will not form, but this threshold varies with the type of water source and appears impractical to control (Krasner, Glaze, Weinberg, Daniel, Najm 1993). Other approaches to limit bromate formation include reduction of ozone dose supplied to water and/or reduction of the water pH. However, these approaches could result in ozonation not meeting its treatment objective, additional chemicals being added to the water to control pH, and increased potential for higher levels of brominated organic byproducts as a result of pH reduction (Yang et al. 2017). Other treatment methods, based on physical means, have also been used to meet the limitation of bromate concentration such as ion exchange process using anion exchange resin, adsorption on granular ferric hydroxide, reduction by granular/powdered activated carbon, reduction by zero-valent ion, filtration by reverse osmosis membrane, UV irradiation and acid-washed aluminum scrap (Zhang et al. 2016; Lin, Lin, Lien 2017; Yang, Dong, Jiang, Wang, Liu 2019a). Bhatnagar et al. (2009) attempted to remove bromate using adsorption on granular ferric hydroxide (GFH) and studied the effect of various experimental parameters such as effect of initial bromate concentration, effect of contact time, temperature and pH (Bhatnagar et al. 2009). It is reported that 75% bromate adsorption was achieved by GFH in 5 min and equilibrium was achieved within 20 min (Bhatnagar et al. 2009). Another method for bromate removal is to use acid-washed zero-valent aluminum, in which zero-valent aluminum (ZVAl) is prepared from aluminum powder washed with acids (Lin and Lin, 2016). In this process, the bromate is reduced to bromide and partially adsorbed to the surface of ZVAl (Lin and Lin, 2016). A hybrid coagulation-nanofiltration process was also studied to remove bromide and bromate, in which two types of membranes (NF-270 and NF-90) and two types of coagulants (alum and ferrous sulfate) were used (Listiarini, Tor, Sun, Leckie 2010). It was observed that bromide could not be efficiently removed by this process, whereas bromate was reduced to bromide

(Listiarini, Tor, Sun, Leckie 2010). Adsorption by powdered activated carbon (PAC) has also been used to remove bromate but with varying efficiencies (Wang et al. 2010). Out of these techniques, ion exchange appears a more desirable approach for bromate control due to its several advantages over other treatment methods. It is very simple in operation, very effective, environment-friendly and relatively inexpensive. Ion exchange (IX) is a reversible process in which undesirable ions in aqueous solution are transferred to a solid medium (i.e., ion exchange resin), which in return releases the ions of same polarity upon regeneration.

In this work, an IX process was effectively used to remove bromate from water. The study has particularly evaluated the performance of a strong-base anion (SBA) ion exchange resin through batch and fixed-bed column experiments. In batch studies, the kinetics and isotherm of the IX process were experimentally determined and described using suitable model equations. The fixed-bed experiments were conducted to examine the column performance through breakthrough curves. Particularly, this study used for the first time a modified equation of the Bohart and Adams model, which takes into account of the non-symmetry of the breakthrough curves and flow channeling, to describe the experimental breakthrough curves. The equilibrium and kinetic parameters determined in this study are useful for optimizing and scaling-up the operation.

Materials and methods

Materials

Stock solutions of bromate at different concentrations were prepared by dissolving a calculated quantity of reagent grade solid sodium bromate (99+%, Fisher Scientific, UK) in distilled water. The experiments were carried out in triplicates and averaged data are presented here. Strong basic anion exchange resin with type I gel matrix (MERCK 104767 ion exchange III) was used in this study. The resin contains solvent and a separating agent (ammonia) and uses hydroxide (OH^-) as the exchange ion. Other characteristics of the resin include appearance: pale brown to brown; exchange capacity $\geq$ 0.9 (mol/L); particle size 0.3–1.2 mm; and bulk density 650–700 g/L. Fresh resins were rinsed with distilled water before first use.

Analytical methods

The concentration of bromate was analyzed by an ion chromatograph (Dionex Integrion HPIC, Thermo Fisher) consisting of a Dionex AS14A IonPac analytical column (2 × 250 mm) fitted with an IonPac AG14 guard column (2 × 50 mm), an electrolytic suppressor (AERS500, 2 mm), a conductivity detector, a high-pressure pump, and a sample injector. The eluent flow rate was 0.5 mL/min and was made of 8.0 mM sodium carbonate (Na_2CO_3) and 1.0 mM sodium bicarbonate ($NaHCO_3$) solution prepared in MilliQ (18.2 M Ω.cm) water. Chromeleon 7 software was used for data acquisition and analysis. The ion chromatograph was calibrated using bromate standard solutions before running a sample. In addition, the ion exchange resin was characterized using adsorption/desorption of nitrogen at 77 K to determine its surface area and pore properties (Nova 2000e, Quantachrome Instruments, Boynton Beach, FL, USA). The Brunauer–Emmett–Teller (BET) model was used to determine the surface area and the pore size properties were determined using the BJH method. The Quantachrome NovaWin software was used for data acquisition and analysis. Initially the sample was degassed with a vacuum pump and heated with a mantle pocket at 100 °C for 3 hours to remove any impurities such as water. The samples were weighed before and after the degassing process.

Batch experiments

Batch ion exchange processes have little importance in industrial applications, but are, as applied in this study, of considerable significance in the evaluation of kinetic mechanisms and determination of isotherms.

Ion exchange kinetics

The kinetics of bromate removal by ion exchange were analyzed using fixed dosages of 0.05 g of resin in 40 mL of bromate solution at different initial concentrations. The ion exchange and solution were mixed using a Stuart™ Rotator Disk (SB3, Fisher Scientific) at a rotating speed of 40 rpm at room temperature. Samples were collected and analyzed for bromate concentration at definite time intervals. The bromate uptake at a given time, t (q, mg/g) was calculated by Equation 1, which results from a mass balance, assuming that all the mass of bromate removed from the aqueous solution was transferred to the resin:

$$q = \frac{(C_0 - C_t) \times V}{m} \qquad [1]$$

where, C_0 and C_t (mg/L) are the bromate concentrations in solution at the initial and at a given time t, respectively, m is the mass of ion exchange resin (g), and V is the volume of solution (L).

The experiment was carried out until no change in concentration was observed and the value of C_t reached

a constant value equal to C_e (i.e., equilibrium). Eq. 1 was used to calculate the bromate uptake at equilibrium, q_e (mg/g) by taking C_t equal to C_e.

Ion exchange isotherms

Batch experiments using different resin masses of 0.01 g, 0.025 g, 0.05 g and 0.1 g added separately to 40 mL solution at initial concentration of 20 mg BrO_3^-/L were performed to determine the isotherms of bromate ion exchange in the anion exchange resin. The contact time between resin and the solution was set to 3 hours, a time that was sufficient to reach equilibrium as obtained in the kinetics studies.

Fixed-bed breakthrough curves

Fixed-bed ion exchange experiments were performed using an ion exchange unit (CE 300 Ion Exchange Unit, Gunt, Germany). This unit consists of two transparent columns (i.d. 21.2 mm, total length 40 cm) made up of PVC material screwed onto a panel, a pump, a variable area flow meter with a float, and a set of valves to direct the flow as required (in this study, the column was fed from the top). The flow rate of feed solution, the ion exchange mass (i.e., bed height), and the feed bromate concentration were varied to study their effects on the breakthrough curve. Typically, these variables were: mass of ion exchange of 5 g (height of 1.2 cm); bromate concentration of 100 mg/L (0.782 mM); and a flow rate of 70 mL/min. The effluent samples were collected at the outlet of the column at specific time intervals and their bromate concentration was analyzed by the ion chromatograph.

Mathematical models

Ion exchange kinetics

The kinetics of mass transfer play an important part in determining the performance of ion exchange operations. The ion exchange between the solution and the resin involves diffusion through a film of the solution enveloping the resin beads (i.e., film diffusion) followed by transport and diffusion within the resin network (i.e., particle diffusion). The slower of these processes determines the rate of ion exchange. Generally, film diffusion is the rate-controlling step at low concentrations, while particle diffusion is the rate-controlling step at high concentrations. Understanding of ion exchange kinetics is extremely important for good performance since, for example in fixed-bed operation, the feed rate of the ion to exchange has to match with the exchange rate of ions. The latter being influenced by ions diffusion coefficients, resin type and structure, selectivity, particle size, and

relative velocities (Slater 1991). Several mathematical equations have been developed to calculate the rate of ion exchange for film diffusion and particle diffusion and those suitably used in this study are described below.

Liquid film diffusion. The liquid film diffusion is applicable when the transfer rate of the solute through the liquid film surrounding the ion exchange particles is the slowest process determining the kinetics of the overall mass transfer rate. The equation for the liquid film diffusion is given by Eq. 2 (Boyd, Adamson, Myers 1947).

$$Ln\left(\frac{q_e}{q_e - q_t}\right) = k_f t \qquad [2]$$

Where q_t is the uptake at a given time t, q_e is the equilibrium uptake, and k_f (min^{-1}) is the film diffusion rate coefficient. A plot of LHS of Eq. 2 vs t should lead to a straight line with a slope equal to k_f.

Particle diffusion. A simple and practical explicit expression for the change of q/q_e as function of time was suggested by Helfferich and Plesset (Helfferich and Plesset, 1957) for the case of particle diffusion control (Eq. 3). This equation is an approximation of the numerical solution, within an error of ±6%, of a model based on ionic diffusion processes and the Nernst–Planck equations taking into account of the differences in diffusivities of exchanging ions.

$$\frac{q(\tau)}{q_e} = \left(1 - exp\left[\pi^2\left(f_1\tau + f_2\tau^2 + f_3\tau^3\right)\right]\right)^{0.5} \qquad [3]$$

where the coefficients f_1, f_2, and f_3 are functions of the ratio $a = D_A/D_B$ and are given by:

$$f_1 = \left(-0.570 - 0.430a^{0.775}\right)^{-1};$$
$$f_2 = \left(0.260 + 7.82a\right)^{-1}; f_3 = \left(-0.165 - 0.177a\right)^{-1};$$

$\tau = D_A t/r$; D_A and D_B are the molecular diffusion coefficients of ions A and B respectively; A is the counter ion initially in the resin and B is the counter ion in solution to exchange (in our case, A = OH^- and, B = BrO_3^-); r is the beads radius.

Ion exchange isotherms

The ion exchange of bromate could be described by the following equilibrium reaction presented in Eq. 4; where R is the resin:
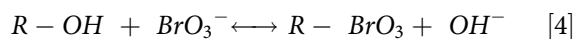
$$R - OH + BrO_3^- \longleftrightarrow R - BrO_3 + OH^- \qquad [4]$$

According to the law of mass action, the equilibrium coefficient, K, can be given by Eq. 5, from which Eq. 6

was derived to represent the isotherm equation of q_e vs C_e at equilibrium.

$$K = \frac{[R - BrO_3][OH^-]}{[R - OH][BrO_3^-]} \quad [5]$$

$$q_e = \frac{\alpha C_e}{1 + \beta C_e} \quad [6]$$

Where α and β are two parameters that depend on the resin capacity, Q_m, the equilibrium coefficient K, and the total solution concentration, C_0, given by the relations: $\alpha = KQ_m/C_0$ and $\beta = (K - 1)/C_0$; and $C_0 = \left[BrO_3^-\right]_0 + [OH^-]_0$.

Eq. 7 gives the equation of the well-known Langmuir model and the relationship between the parameters of the equilibrium equation determined from the law of mass action and the Langmuir constants K_L and q_{maxL} are given by Eq. 8 and 9.

$$q_e = \frac{q_{maxL}K_L C_e}{1 + K_L C_e} \quad [7]$$

where: K_L (L/mg) represents the Langmuir isotherm constant and q_{maxL} (mg/g) is the maximum ion exchange capacity.

$$K = K_L C_0 + 1 \quad [8]$$

$$Q_m = \frac{K - 1}{K} q_{maxL} \quad [9]$$

Fixed-bed column modeling (modified Bohart and Adams model)

The breakthrough curve is commonly used to describe the performance of fixed-bed columns. It necessitates careful analysis and assessment of the experimental data to predict the effect of the various operational parameters such as flow rate, inlet concentration, and characteristics of the bed. A modified equation (both in terms of channeling and asymmetry of the curve) of the widely used Bohart and Adams equation was used in this study to describe the bromate breakthrough curves at different inlet concentrations, flow rates and bed heights. The asymmetry of the breakthrough curves was modeled using the *n*-order Bohart–Adams model (Hu, Pang, Wang, Yang, Liu 2021) while channeling was accounted for through measurement of the column outlet concentration at time zero. For this, it was assumed that channeling reduces the liquid flow rate that is effectively in contact with the resin beads by a factor (C_0 -C_{eff0})/C_0 and C would then rises with time from C_{eff0} to C_0 as ion exchange progresses; where C_{eff0} is a bromate concentration determined by the intersection of the asymptote line of the lower part of the breakthrough curve and the y-axis (Figure 1).

Results and discussion

Resin characterization

For the BET adsorption/desorption analysis, two samples of the MERCK 104767 ion exchange III used in this study were prepared including unaltered resin and crushed resin. The results showed that the surface area of the unaltered resin and the crushed resin had a similar
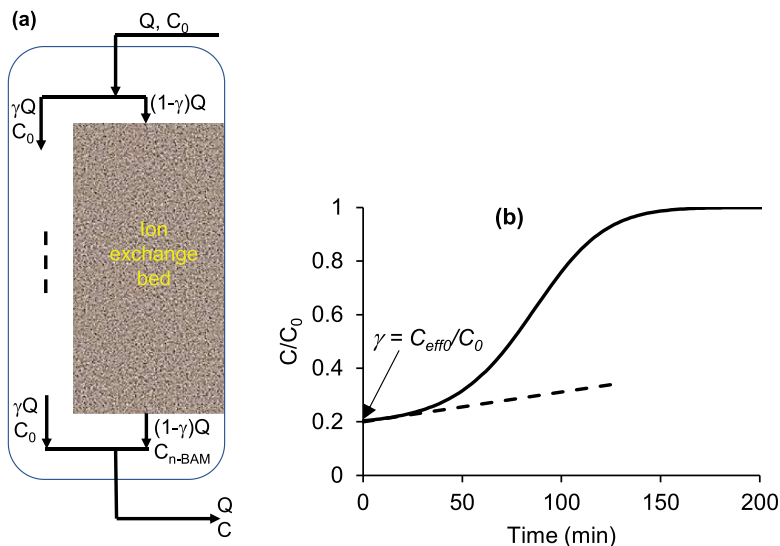

Figure 1. (a) Schematic representation of the ion exchange fixed-bed model, and (b) representation for the determination of C_{eff0}.

value of 25.0 ± 3.1 m^2/g. This surface area value was found comparable to other ion exchange resins such as the macroporous VPOC1065 (24.6 m^2/g) (Ijzer, Vriezekolk, Rolevink, Nijmeijer 2015) and FO Dowex resin (21.6 m^2/g) (Tandorn, Arqueropanyo, Naksata, Sooksamiti 2017). In addition, the cryogenic nitrogen adsorption desorption cycle was found to follow Type III isotherm, which is characteristic of a weak adsorbate-adsorbent interaction and corresponds to multimolecular adsorption. The resin pore volume analysis using the BJH method gave a pore volume of 0.019 ± 0.004 cm^3/g and a pore diameter of 3.48 ± 0.02 nm. These results are comparable to other studies (Ijzer, Vriezekolk, Rolevink, Nijmeijer 2015; Yang et al. 2019b) and indicate that the ion exchange is mesoporous (Yang et al. 2019b).

Batch experiments

Bromate ion exchange kinetics

The kinetics of bromate ion exchange were evaluated in batch experiments using an initial bromate concentration of 20 mg/L and 0.05 g of resin in 40 mL of solution. The concentration of bromate in aqueous solution was measured at different times and typical results are plotted in Figure 2. The results show an initial rapid removal of bromate followed by a progressively slowing change in concentration to a final value (C_f) after about one hour.

The bromate uptake, q was calculated by Eq. 1 and the corresponding plot of q vs time is also shown in Figure 2. It can be clearly seen that the process of bromate ion exchange was accomplished in three stages. At the initial stage, the ion exchange resin exhibited a rapid uptake of bromate within the first 2 min. Thereafter, the bromate uptake was slowly increased as the time elapsed from 2 to 60 min. Finally, there was no significant change in the uptake after 60 min, signaling that equilibrium was rea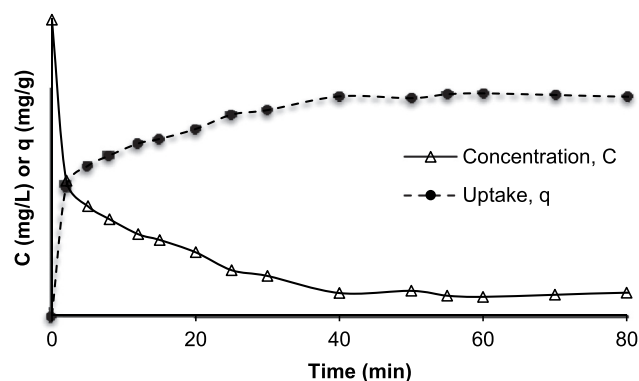ched. Initially, the resin surface has sufficient anions available to exchange with bromate, leading to rapid increase in bromate uptake due to high concentration gradient between bromate solution and the resin surface which accelerates the diffusion process of bromate from the liquid phase to the solid phase, hence the observed initial sharp increase in uptake (Yan, Du, Li, Yu, Tang 2015). As the process continues, the sites available on the resin surface decrease, thereby resulting in smaller concentration gradient and a slowdown of the diffusion process. This results in the observed decrease in bromate removal rate. Finally, the equilibrium was achieved after 60 min and the equilibrium exchange capacity of the resin material (q_e) was reached. There was no significant change in bromate uptake in the following 24 hours, which confirms further that equilibrium was reached after about 1 h. The rates of ion exchange at different initial concentrations were also determined, and the results show that as the initial concentration increased from 10 to 65 mg/L, the equilibrium time also increased from 20 to 80 min (Figure 3). The bromate uptake by the IX resin was also increased with increasing the initial concentration, which is in agreement with other studies (Ding, Deng, Wu, Han 2012).

Modeling of the ion exchange kinetics

The study of ion exchange kinetics is important for designing ion exchange systems and understanding the ion exchange mechanisms (Yan, Du, Li, Yu, Tang 2015). To quantitatively clarify the ion exchange mechanism, both the liquid film diffusion and particle diffusion kinetic models were applied to the batch experimental data. These kinetic models were used to determine the rate of ion exchange process, which is an important factor in the design of ion exchange facilities. As depicted in Figure 4a, the results showed higher rates
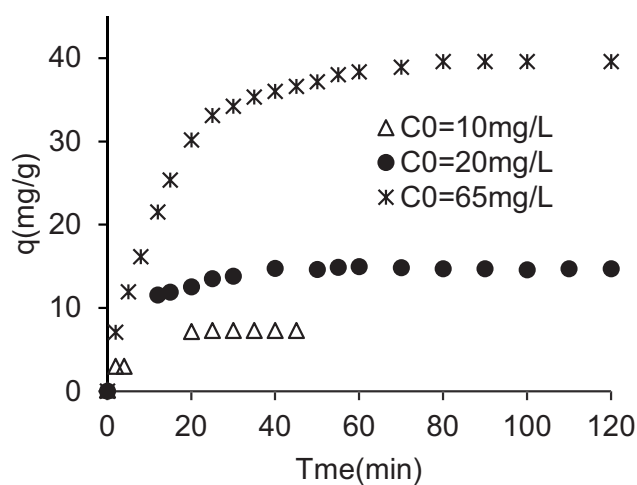
Figure 2. Bromate uptake kinetics (C_0 = 20 mg/L, 0.05 g of resin, 40 mL of solution).

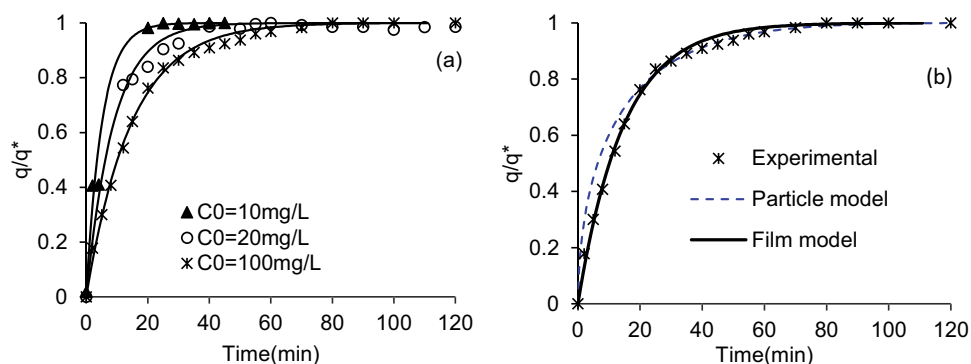**Figure 3.** Effect of initial bromate concentration on bromate uptake.

Figure 4. Effect of initial bromate concentration on the ion exchange kinetics (a) film control model; (b) particle diffusion model compared to film control (C_0 = 100 mg/L).

within the first 2 min, followed by slower rates until the equilibrium is reached after about 60 min. The fitting of the experimental results with both film control and particle diffusion control models showed that the film control gives better fit than the particle diffusion control model (Figure 4b). This is consistent with the fact that particle control and film control govern ion exchange processes in concentrated solutions and solutions at low concentrations, as is the case in this study, respectively. The effect of initial bromate concentration on the film diffusion rate coefficient, k_f, is shown in Table 1. As shown in the table, the value of k_f inversely varies with the initial concentration, which is in agreement with other studies (Allen, Gan, Matthews, Johnson 2005; Guo et al. 2013). Figure 4b indicates that, within the studied concentration range, the film control model fits the experimental data well for almost the entire ion exchange process including the rapid initial phase and the subsequent more slower phase. Table 1 also shows the values of the model parameter q_e obtained at the various initial concentrations, which increases as function of C_0. The values of q_e are the equilibrium values at the final concentrations obtained at the end of the ion exchange process. The values of q_e, calculated by the film model fitting to the experimental data, are found close to the experimental values determined from the isotherm study. Hence, it can be concluded that this experimental and theoretical data can be used to favorably explain the bromate exchange process on the anion exchange III resin. In addition, since the values of the theoretical equilibrium uptake, q_e, were found close to the

experimental values, the bromate removal according to the film control model is further demonstrated.

Ion exchange isotherms

Isotherms describe the capacity of interaction between the liquid and solid phase in the ion exchange systems. The isotherm models are very useful tools for the analysis of ion exchange mechanisms, resin properties, for example, exchange capacity, affinity of resin, and so on (Yan, Du, Li, Yu, Tang 2015). In this study, the equilibrium exchange capacity of the resin was studied as a function of equilibrium bromate concentration by applying the Freundlich and Langmuir isotherm models to the experimental data. The most suitable model was selected using the best fit method based on minimizing the sum of squared residuals between experimental and model values. The equations and parameters of each model are shown in Table 2. Figure 5 clearly shows that the Langmuir model fitted better the experimental data than the Freundlich model, which is also supported by the higher R^2 value obtained for the Langmuir model (Table 2). The Freundlich model is applicable to ion exchange processes that take place on heterogeneous resin surfaces and follow multilayer adsorption (Yan, Du, Li, Yu, Tang 2015). In contrast, the Langmuir isotherm expresses a homogeneous resin surface and the removal of bromate was in the form of monolayer on the resin surface, which is expected for ion exchange since the process develops based on one equivalent exchange

Table 1. Effect of initial concentration on the parameters of the film model.

C_0 (mg BrO$_3^-$/L)	q_e (mg/g)	k_f (s^{-1})
10	7.3	0.0033
20	14.9	0.0019
65	39.6	0.0011

Table 2. Parameters of Freundlich and Langmuir isotherm models.

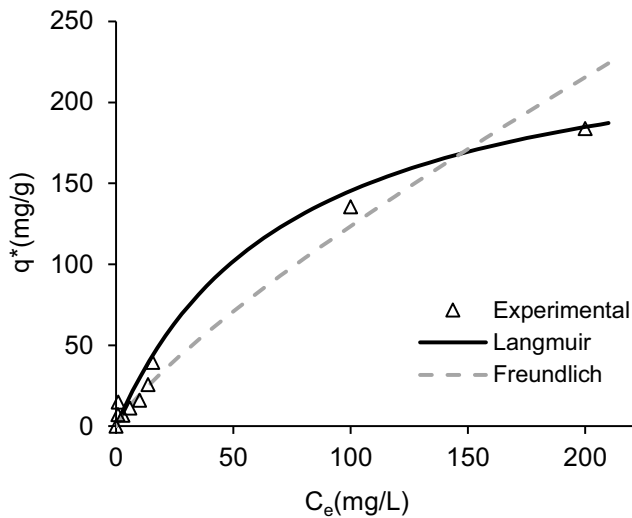| Types of isotherm	Parameters	Values
Freundlich isotherm	K_F (L/g)	3.073
$q_e = K_F C_e^{\frac{1}{n}}$	1/n	0.8022
	R^2	0.9806
Langmuir isotherm	K_L (L/mg)	0.00825
$q_e = \frac{q_{max} K_L C_e}{1 + K_L C_e}$	q_{max} (mg/g)	296.66
	R_L	0.37 to 0.71
	R^2	0.995

Figure 5. Langmuir and Freundlich isotherms for bromate ion exchange.

of one equivalent between the two phases and is in accordance with other studies (Yan, Du, Li, Yu, Tang 2015). The Langmuir model also served to calculate the maximum exchange capacity (q_{max}), achieved after the saturation of resin surface, and in our study its value was found 296.66 mg/g (~1.3 meq/mL resin). This maximum adsorption capacity is within the same range (>300 mg/g) of that reported in Yang et al. (2019b). The important characteristics of the Langmuir isotherm can be stated by the dimensionless number known as the separation factor R_L, which is defined as (Naushad, Khan, Alothman, Awual 2016):

$$R_L = \frac{1}{1 + K_L C_0} \qquad [10]$$

Where, C_0 (mg/L) is the initial bromate concentration. R_L value indicates whether the isotherm is favorable ($0 < R_L < 1$), linear ($R_L = 1$), unfavorable ($R_L > 1$) or irreversible ($R_L = 0$) (Naushad, Khan, Alothman, Awual 2016). The values of R_L for all initial concentrations used in this study were found to vary in the range 0.37 to 0.71 (Table 2), which implies favorable isotherm for all concentrations studied.

Effect of temperature

The effect of temperature on bromate exchange by the resin was evaluated at the temperatures 10, 25 and 40 C and the solution initial concentration was 20 mg/L. The values of the equilibrium constant, K, were determined at each temperature. Theoretically, the effect of temperature on K can be described by the van't Hoff equation (Eq. 11) leading to the determination of the thermodynamic parameters including Gibbs free energy change (ΔG^o), standard enthalpy change (ΔH^o), and standard

entropy change (ΔS^o). The calculated values of ΔG^o were negative (−6.8 to −3.4 kJ/mol) at all temperatures indicating that the ion exchange of bromate was spontaneous and thermodynamically feasible. In addition, as temperature increased from 10 to 40 C, ΔG became more negative implying that higher temperatures favored the sorption of bromate on the resin. The values of ΔH^o and ΔS^o were determined from the slope and intercept of the straight line obtained by plotting $Ln(K_L)$ versus $1/T$ (Eq. 12) and their values were 28.6 kJ/mol and 113 J/(mol.K), respectively. The positive sign of the standard enthalpy value indicates that the process was endothermic, meaning that as temperature increased, the bromate uptake also increased. This finding is consistent with the discussion for ΔG^o and is in agreement with other studies who also showed that increasing temperature increased ion exchange uptake (Guesmi, Hannachi, Hamrouni 2010; Xu et al. 2018). Besides, the positive sign of ΔS^o indicates that the randomness increased during bromate sorption. Xu et al. (2018) have also found that the randomness increased during the sorption of bromate ions on the magnetic resin they studied and suggested that this may due to lower affinity of bromate for the active sites. The values of ΔH^o and ΔS^o obtained in our study are also comparable to other studies (Chaabouni, Guesmi, Louati, Hannachi, Hamrouni 2015).

$$\Delta G^o = \Delta H^o - T\Delta S^o = -RTln(K_L) \qquad [11]$$

$$ln(K_L) = -\left(\frac{\Delta H^o}{R}\right)\frac{1}{T} + \frac{\Delta S^o}{R} \qquad [12]$$

Fixed-bed column tests

Breakthrough curve

The fixed-bed column experiments were made at an inlet bromate concentration of 100 mg/L and a constant downward flow rate of 70 mL/min. As the feed water was passing through the resin bed, ion exchange was taking place. The bromate concentration at the outlet of the column was periodically measured and a typical breakthrough curve is presented in Figure 6a. The breakthrough curve shows the loading behavior of bromate to be eliminated from the feed solution and is generally expressed in terms of the ratio of the outlet concentration to the inlet concentration (C/C_0) as function of time, t (Nur, Shim, Loganathan, Vigneswaran, Kandasamy 2015). Initially, there was less bromate concentration ($C/C_0 \sim 0.11$) in the effluent followed by a modest increase in concentration until about 80 min before
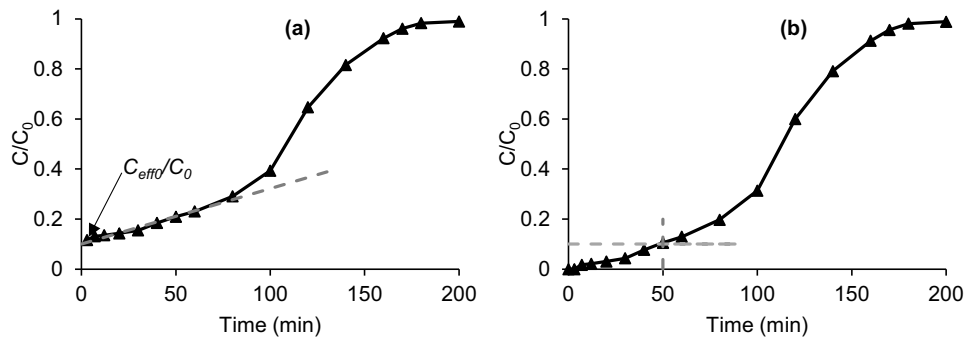
Figure 6. Breakthrough curve for bromate ion exchange in fixed bed (Q = 70 mL/min; C_0 = 100 mg/L, bed height = 1.2 cm). (a) as measured experimentally, (b) corrected for flow channeling.

bromate concentration suddenly increased in the effluent until it reached the equilibrium point, which is marked by $C/C_0 \sim 1$; the equilibrium point, t_e was around 180 min. At time $t \to 0$, the concentration was higher than zero due to water channeling in the void spaces between the spherical resin beads. This means that a fraction of the flow, taken as γ, was not contacting the resin and escapes the column without exchanging bromate in the resin (Figure 6a). A mass balance across the column at $t \to 0$ (Figure 1), leads to $\gamma C_0 = C_{eff0}$, from which γ is simply calculated by Eq. 13. Correcting for channeling, the

breakthrough curve could be presented as in Figure 6b. According to this figure, the breakthrough point (10%) would occur at a time, t_b, of about 50 min. Moreover, the breakthrough curves appear asymmetrical, which means that different mechanisms take place as the bed gets saturated. This implies that traditional fixed-bed models (e.g., Bohart–Adams, Thomas model), which are suitable for symmetrical breakthrough curves, would poorly fit the experimental data. Thus, in this study, we used an n-order Bohart-Adams model, which is more adequate for asymmetric breakthrough curves, to
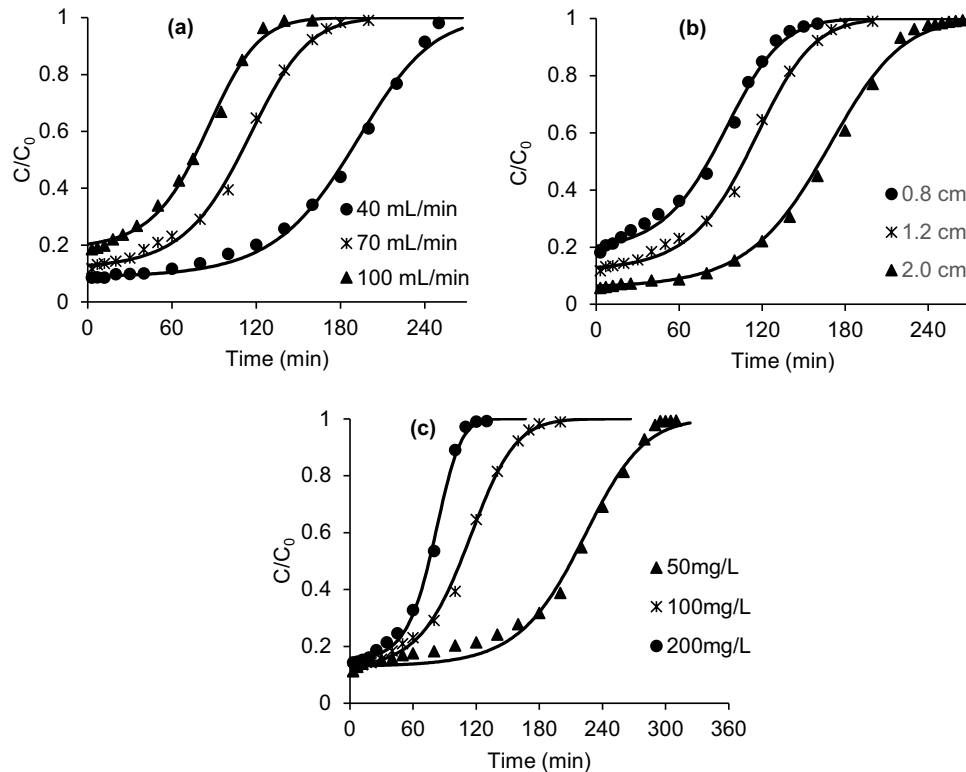

Figure 7. Bromate breakthrough curves at different: (a) flow rates (Z = 1.2 cm, C_0 = 100 mg/L); (b) bed heights (Q = 70 mL/min, C_0 = 100 mg/L); (c) inlet concentrations (Q = 70 mL/min, Z = 1.2 cm); continuous lines are fitting lines by the n-BAM-c model.

describe the experimental data (Hu, Pang, Wang, Yang, Liu 2021).

$$\gamma = \frac{C_{eff0}}{C_0} \qquad [13]$$

Where: γ is the fraction of the flow that does not contact the resin; C_{eff0}, is the measured effluent concentration that bypass ion exchange at t→0; and C_0 is the inlet bromate concentration.

Effects of flow rate, bed height and initial concentration on breakthrough curve

The effects of flow rate, bed height, and inlet concentration on breakthrough curves are shown on Figure 7a–c. The figure shows that the breakthrough of bromate occurred faster at high flow rates, high inlet concentrations, and low bed heights. The breakthrough time, t_b (determined after correcting for channeling) was reduced from 140 to 50 min, as the flow rate increased from 40 to 100 mL/min (Table 3). The time to reach equilibrium was increased significantly at low flow rate (~260 min) and the breakthrough curves became steeper as the flow rate increased, which is in agreement with other studies (Yang et al. 2015). The earlier breakthrough shown by higher flow rate is due to the less contact time between bromate and the resin, caused by the fast movement of the adsorption zone along the resin bed. In other words, bromate did not have sufficient time to fully diffuse into the pores of the resin and therefore, at high flow rate, the solution left the column before sufficient mass transfer took place. Thus, low flow rates are required to have high residence time in the column and achieve high bromate removal. Similarly, low bed height resulted in faster breakthrough time, which increased from 60 to 120 min as the bed height increased from 0.8 to 2 cm. In addition, the throughput volumes of feed solution at breakthrough points (V_b)

were 4.2, 5.6 and 8.4 L for the bed heights of 0.8, 1.2 and 2 cm, respectively (Table 3), implying that with higher bed heights, the removal of bromate is high. Thus, the more contact between bromate in solution and the resin, the better performance of the fixed-bed column (Yang et al. 2015). The effect of concentration revealed that early breakthrough was achieved for higher inlet concentration with the breakthrough times, t_b were 200, 80 and 60 min for concentrations of 50, 100 and 200 mg/L, respectively. The higher the inlet concentration, the steeper the breakthrough curve was. This can be explained by the fact that high concentration corresponds to high concentration gradient which provides a greater mass transfer driving force, implying higher ion exchange rate in the column (Du, Zheng, Wang 2018). Moreover, the values of V_b were increased from 4.2 to 14 L as the concentration decreased from 200 to 50 mg/L.

The effects of flow rate, bed height, and inlet concentration on the fraction of flow that does not contact the resin, γ, due to channeling, was also determined and the results are shown in Table 3. Both flow rate and bed height have a significant effect on γ while the inlet concentration has no important effect. The ratio γ is related to the channeling that occur in the column, with the higher the γ, the higher the channeling, meaning a poor distribution of the flow throughout the resin-packed bed. Channeling would limit the efficiency of the column because only a fraction of the flow would effectively contact the resin. In view of the values of γ (Table 3), it is evident that the channeling effect is more pronounced at high flow rates and low bed heights (i.e., high γ).

Fixed-bed column modeling

To account for the asymmetry of the breakthrough curves, the n-order Bohart and Adams Model

Table 3. Parameters obtained from fixed-bed studies.

Condition	Value	Breakthrough time, t_b (min)	Volume at breakthrough, V_b (L)	Equilibrium time, t_e (min)	$\gamma = \frac{C_{eff0}}{C_0}$	n(-)	a_0(mg/L)	k_n(L^n/ (mg^n.s)	R^2
Flow rate (mL/min)	40	140	5.6	260	0.09	0.891	1.78×10^5	1.24×10^{-5}	0.9986
(C_0 = 100 mg/L;	70	80	5.6	180	0.12	0.895	1.78×10^5	1.70×10^{-5}	0.9992
Z = 1.2 cm)	100	50	5	140	0.19	0.899	1.78×10^5	1.99×10^{-5}	0.999
Bed height (cm)	0.8	60	4.2	160	0.18	0.886	1.78×10^5	2.00×10^{-5}	0.9989
(C_0 = 100 mg/L;	1.2	80	5.6	180	0.12	0.895	1.78×10^5	1.70×10^{-5}	0.9992
Q = 70 mL/min)	2	120	8.4	260	0.06	0.899	1.78×10^5	1.24×10^{-5}	0.9992
Initial Concentration (mg/L)	50	200	14	295	0.13	0.902	1.78×10^5	2.08×10^{-5}	0.9978
(Q = 70 mL/min;	100	80	5.6	180	0.12	0.895	1.78×10^5	1.70×10^{-5}	0.9992
Z = 1.2 cm)	200	60	4.2	120	0.14	0.843	1.78×10^5	2.11×10^{-5}	0.9990

$$\frac{C_{n-BAM}}{C_0} = \frac{1}{\left[1 + na_0^{1-n}C_0^{n-1}\left(\left[\frac{1+(n-1)\frac{k_n a_0 C_0^{n-1}x}{u}}{1+(n-1)k_n a_0^{n-1}C_0 t}\right]^{\frac{1}{n-1}} - \left[\frac{1}{1+(n-1)k_n a_0^{n-1}C_0 t}\right]^{\frac{1}{n-1}}\right)\right]^{\frac{1}{n}}} \quad [14]$$

(n-BAM), which was recently discussed by Hu et al. (2021), was used in this study after being modified to also account for channeling (Figure 1). The equation representing n-BAM is given by Eq. 14 and the modified model that takes account of channeling (n-BAM-c) is given by Eq. 15. In developing this equation, it was assumed that the ratio γ, measured at $t\rightarrow 0$, remains constant (i.e., the channeling effect of the flow does not change over time since the flow and bed height were constant) and the fraction of flow $(1-\gamma)$ homogeneously contacts the ion exchange bed. In the development of the n-BAM, it was assumed that the rate of reaction is a nonlinear decay process with respect to concentration and residual capacity of the adsorbent (Hu, Pang, Wang, Yang, Liu 2021). The model parameter, a_0, which represents the initially available capacity of the ion exchange (mg/L) was determined from the maximum ion exchange capacity and its value was found 1.78×10^5 mg/L. The other model parameters (n, k_n) were determined by fitting the experimental data using the least square method and their values are shown in Table 3 as function of the operating conditions. The calculation was done in MS Excel using the Solver add-in run with the GRG Nonlinear solving method. Figure 7 shows excellent fitting of the experimental results with the n-BAM-c model as also demonstrated by high R^2 values shown in Table 3. Table 3 highlights that the flow rate affects k_n since a change of the flow rate from 40 to 100 mL/min increased k_n by 1.6 times, which indicates that the process is governed by external film mass transfer (Mantovaneli, Ferretti, Simoes, da Silva 2004). This finding is also in agreement with the kinetics study conducted in batch mode (section 3.1.2). The flow rate was also found to increase the parameter, n, but only slightly from 0.891 to 0.899. In addition, Table 3 shows that the bed height has opposite effect to flow rate since k_n was reduced by about a third as the bed height increased from 0.8 to 2 cm. The parameter n slightly increased from 0.886 to 0.899 as the bed height increased, though. Thus, it can be stated that albeit higher bed height and lower flow rate increase residence time in the bed, they reduce the mass transfer rate, which suggests that there is a compromise between

residence time and transfer rates. The effect of inlet concentration on k_n was insignificant but n was slightly reduced from 0.902 to 0.843 as C_0 increased from 50 to 200 mg/L. These results highlight that n-BAM-c provides a powerful fitting quality for asymmetric breakthrough curves that exhibit channeling, whilst adequate use of the model for design and upscaling purposes would require experimental validation of the effect of the operating conditions on the model parameters.

$$\frac{C}{C_0} = \gamma + (1-\gamma)\frac{C_{n-BAM}}{C_0} \quad [15]$$

Where: C_0 is the inlet bromate concentration (mg/L), C_{n-BAM} is the concentration calculated by the n-order Bohart and Adams Model (mg/L) (Eq. 14), C is the outlet concentration (mg/L), γ is the ratio of channeled flow, a_0 is the initially available capacity of the ion exchange (mg/L), k_n is the n-order Bohart-Adams rate constant ($L^n/(mg^n.s)$), and n is the order of BAM.

Removal of bromate with ion exchange could offer an elegant way to deal with the bromate issue caused by the ozonation of bromide-containing waters. The use of ion exchange fixed-bed columns implies that the regeneration of the bed is an additional step required to allow re-using the resin once it is saturated. For this, the exhausted SBA resin can be regenerated using a concentrated solution of sodium hydroxide (NaOH) (Naushad, Khan, Alothman, Awual 2016). The NaOH solution is flown through the column to allow adequate contact with the resin particles until the adsorbed bromate ions are exchanged with the hydroxide ions. The bed is then rinsed gradually by the introduction of dilution water before another cycle of bromate removal is made.

Conclusions

In this study, a strong-base anion exchange III resin was used to remove bromate from water in batch and fixed-bed operations; bromate being a regulated by-product of ozonation. The bromate ion exchange process was characterized by a very rapid uptake at the start of the

operation followed by a slower uptake before reaching equilibrium. The equilibrium time was found to vary with the initial bromate concentration from 20 to 80 min at initial concentrations varying from 10 to 65 mg/L. In the IX kinetics study, both the liquid film diffusion and particle diffusion kinetic models were applied to the batch experimental data. The fitting of the experimental results with both film and particle diffusion control models showed that the film control gives better fit than the diffusion control model and the values of the theoretical equilibrium uptake, q_e, were in line with the experimental results. The isotherm studies revealed that the Langmuir model satisfied well the experimental data than the Freundlich model. This suggests that the resin surface was homogeneous, and the exchange process took place in the form of a monolayer. The fixed-bed studies revealed that the breakthrough time (t_b) decreased with either increasing the flow rate or increasing the inlet bromate concentration. However, an increase in the bed height extended the breakthrough time. These results suggest that the bromate removal can be improved with lower flow rate and higher bed heights but due to channeling and the asymmetric nature of the breakthrough curve, the impact on mass transfer should be observed. A modified equation of the n-order Bohart and Adams model was developed in this study, taking account of flow channeling and asymmetry of the breakthrough curves (n-BAM-c). The results showed that the n-BAM-c model fitted well the experimental data and the effects of the main operating conditions (inlet concentration, flow rate, and bed height) on the model parameters were determined. It was suggested that the n-BAM-c model could provide a powerful tool for design and upscaling of ion exchange processes. Overall, this study demonstrated that the strong-base anion exchange III was suitable for bromate removal and has the potential to remove bromate from water efficiently at large scale upon careful upscaling of results.

Disclosure statement

References

Allen, S.J., Q. Gan, R. Matthews, and P.A. Johnson. 2005. "Kinetic Modeling of the Adsorption of Basic Dyes by Kudzu." *Journal of Colloid and Interface Science* 286 (1): 101–09. doi:10.1016/j.jcis.2004.12.043

Arvai, A., S. Jasim, and N. Biswas. 2012. "Bromate Formation in Ozone and Advanced Oxidation Processes." *Ozone: Science & Engineering* 34 (5): 325–33. doi:10.1080/01919512.2012.713834

Bhatnagar, A., Y. Choi, Y. Yoon, Y. Shin, B.-H. Jeon, and J.-W. Kang. 2009. "Bromate Removal from Water by Granular Ferric Hydroxide (GFH)." *Journal of Hazardous Materials* 170 (1): 134–40. doi:10.1016/j.jhazmat.2009.04.123

Boyd, G.E., A.W. Adamson, and L.S. Myers. 1947, "The Exchange Adsorption of Ions from Aqueous Solutions by Organic Zeolites. II. Kinetics." *Journal of the American Chemical Society* 69 (11): 2836–48. doi:10.1021/ja01203a066

Chaabouni, A., F. Guesmi, I. Louati, C. Hannachi, and B. Hamrouni. 2015. "Temperature Effect on Ion Exchange Equilibrium between CMX Membrane and Electrolytes Solutions." *Journal of Water Reuse and Desalination* 5 (4): 535–41. doi:10.2166/wrd.2015.008

Collivignarelli, M.C., A. Abbà, I. Benigna, S. Sorlini, and V. Torretta. 2018. "Overview of the Main Disinfection Processes for Wastewater and Drinking Water Treatment Plants." *Sustainability* 10 (1): 86. doi:10.3390/su10010086

Delker, D., G. Hatch, J. Allen, B. Crissman, M. George, D. Geter, S. Kilburn, T. Moore, G. Nelson, B. Roop, et al. 2006. "Molecular Biomarkers of Oxidative Stress Associated with Bromate Carcinogenicity." *Toxicology* 221 (2–3): 158–65. doi:10.1016/j.tox.2005.12.011

Ding, L., H.P. Deng, C. Wu, and X. Han. 2012. "Affecting Factors, Equilibrium, Kinetics and Thermodynamics of Bromide Removal from Aqueous Solutions by MIEX Resin." *Chemical Engineering Journal* 181:360–70. doi: 10.1016/j.cej.2011.11.096.

Du, Z.L., T. Zheng, and P. Wang. 2018. "Experimental and Modelling Studies on Fixed Bed Adsorption for Cu(II) Removal from Aqueous Solution by Carboxyl Modified Jute Fiber." *Powder Technology* 338:952–59. doi: 10.1016/j.powtec.2018.06.015.

Fang, J.Y., and C. Shang. 2012. "Bromate Formation from Bromide Oxidation by the UV/persulfate Process." *Environmental Science & Technology* 46 (16): 8976–83. doi:10.1021/es300658u

Guesmi, F., C. Hannachi, and B. Hamrouni. 2010. "Effect of Temperature on Ion Exchange Equilibrium between AMX Membrane and Binary Systems of Cl−, NO− 3 and SO2− 4 Ions." *Desalination and Water Treatment* 23 (1–3): 32–38. doi:10.5004/dwt.2010.1837

Guo, H., Y. Ren, X. Sun, Y. Xu, X. Li, T. Zhang, J. Kang, and D. Liu. 2013. "Removal of Pb2+ from Aqueous Solutions by a high-efficiency Resin." *Applied Surface Science* 283:660–67. doi: 10.1016/j.apsusc.2013.06.161.

Helfferich, F., and M.S. Plesset. 1957. *Ion Exchange Kinetics - a Nonlinear Diffusion Problem*. California: Office of Naval Research.

Hu, Q.L., S.Y. Pang, D. Wang, Y.H. Yang, and H.Y. Liu. 2021. "Deeper Insights into the Bohart-Adams Model in a Fixed-Bed Column." *Journal of Physical Chemistry B* 125 (30): 8494–501. doi:10.1021/acs.jpcb.1c03378

Huang, X., Y. Deng, S. Liu, Y. Song, N. Li, and J. Zhou. 2016. "Formation of Bromate during ferrate(VI) Oxidation of Bromide in Water." *Chemosphere* 155:528–33. doi: 10.1016/j.chemosphere.2016.04.093.

Huang, X., N. Gao, and Y. Deng. 2008. "Bromate Ion Formation in Dark Chlorination and ultraviolet/chlorination Processes for bromide-containing Water." *Journal of Environmental Sciences* 20 (2): 246–51. doi:10.1016/S1001-0742(08)60038-8

Ijzer, A.C., E. Vriezekolk, E. Rolevink, and K. Nijmeijer. 2015. "Performance Analysis of Aromatic Adsorptive Resins for the Effective Removal of Furan Derivatives from Glucose." *Journal of Chemical Technology and Biotechnology* 90 (1): 101–09. doi:10.1002/jctb.4294

JRC. 2016. "Bromate in Drinking Water: JRC Finds New Testing Method Fit for Purpose. https://ec.europa.eu/jrc/en/news/bromate-drinking-water-jrc-finds-new-testing-method-fit-purpose-8292".

Krasner, S.W., W.H. Glaze, H.S. Weinberg, P.A. Daniel, and I. N. Najm. 1993. "Formation and Control of Bromate during Ozonation of Waters Containing Bromide." *Journal - American Water Works Association* 85 (1): 73–81. doi:10.1002/j.1551-8833.1993.tb05923.x

Lin, K.-Y.A., and C.-H. Lin. 2016. "Simultaneous Reductive and Adsorptive Removal of Bromate from Water Using acid-washed zero-valent Aluminum (Zval)." *Chemical Engineering Journal* 297:19–25. doi: 10.1016/j.cej.2016.03.136.

Lin, K.-Y.A., J.-Y. Lin, and H.-L. Lien. 2017. "Valorization of Aluminum Scrap via an acid-washing Treatment for Reductive Removal of Toxic Bromate from Water." *Chemosphere* 172:325–32. doi: 10.1016/j.chemosphere.2017.01.040.

Listiarini, K., J.T. Tor, D.D. Sun, and J.O. Leckie. 2010. "Hybrid coagulation–nanofiltration Membrane for Removal of Bromate and Humic Acid in Water." *Journal of Membrane Science* 365 (1): 154–59. doi:10.1016/j.memsci.2010.08.048

Liu, C., U. von Gunten, and J.-P. Croué. 2012. "Enhanced Bromate Formation during Chlorination of Bromide-Containing Waters in the Presence of CuO: Catalytic Disproportionation of Hypobromous Acid." *Environmental Science & Technology* 46 (20): 11054–61. doi:10.1021/es3021793

Mansouri, L., C. Tizaoui, S.U. Geissen, and L. Bousselmi. 2019. "A Comparative Study on Ozone, Hydrogen Peroxide and UV Based Advanced Oxidation Processes for Efficient Removal of Diethyl Phthalate in Water." *Journal of Hazardous Materials* 363:401–11. doi: 10.1016/j.jhazmat.2018.10.003.

Mantovaneli, I.C.C., E.C. Ferretti, M.R. Simoes, and C.F. da Silva. 2004. "The Effect of Temperature and Flow Rate on the Clarification of the Aqueous stevia-extract in a fixed-bed Column with Zeolites." *Brazilian Journal of Chemical Engineering* 21 (3): 449–58. doi:10.1590/S0104-66322004000300009

Naushad, M., M.R. Khan, Z.A. Alothman, and M.R. Awual. 2016. "Bromate Removal from Water Samples Using Strongly Basic Anion Exchange Resin Amberlite IRA-400: Kinetics, Isotherms and Thermodynamic Studies." *Desalination and Water Treatment* 57 (13): 5781–88. doi:10.1080/19443994.2015.1005157

New York State Department of Health. 2017. "Bromate in Drinking Water - Information Fact Sheet". https://www.health.ny.gov/environmental/water/drinking/bromate.htm".

Nur, T., W.G. Shim, P. Loganathan, S. Vigneswaran, and J. Kandasamy. 2015. "Nitrate Removal Using Purolite A520E Ion Exchange Resin: Batch and fixed-bed Column Adsorption Modelling." *International Journal of Environmental Science and Technology* 12 (4): 1311–20. doi:10.1007/s13762-014-0510-6

Slater, M.J. 1991. *Principles of Ion Exchange Technology*. Oxford, UK: Butterworth-Heinemann.

Tandorn, S., O.-A. Arqueropanyo, W. Naksata, and P. Sooksamiti. 2017. "Preparation of Anion Exchange Resin Loaded with Ferric Oxide for Arsenic (V) Removal from Aqueous Solution." *International Journal of Environmental Science and Development* 8 (6): 399–403. doi:10.18178/ijesd.2017.8.6.985

Tizaoui, C., N. Grima, and N. Hilal. 2011. "Degradation of the Antimicrobial Triclocarban (TCC) with Ozone." *Chemical Engineering and Processing-Process Intensification* 50 (7): 637–43. doi:10.1016/j.cep.2011.03.007

Tizaoui, C., and Y.M. Zhang. 2010. "The Modelling of Ozone Mass Transfer in Static Mixers Using Back Flow Cell Model." *Chemical Engineering Journal* 162 (2): 557–64. doi:10.1016/j.cej.2010.05.061

Tynan, P., D. Lunt, and J. Hutchison. 1993. "The Formation of Bromate during Drinking Water Disinfection". http://dwi.defra.gov.uk/research/completed-research/reports/dwi0137.pdf

VanBriesen, J.M. n.d. "Potential Drinking Water Effects of Bromide Discharges from Coal-Fired Electric Power Plants". https://www3.epa.gov/region1/npdes/merrimackstation/pdfs/Comments2RevisedDraftPermit/VanBriesenReport.pdf ".

Wang, L., J. Zhang, J. Liu, H. He, M. Yang, J. Yu, Z. Ma, and F. Jiang. 2010. "Removal of Bromate Ion Using Powdered Activated Carbon." *Journal of Environmental Sciences* 22 (12): 1846–53. doi:10.1016/S1001-0742(09)60330-2

WHO. 2005. "Bromate in Drinking-water: Background Document for Development of WHO Guidelines for Drinking-water Quality. https://www.who.int/water_sanitation_health/dwq/chemicals/bromate260505.pdf .

Xu, Z.M., D.X. Han, Y. Li, P.L. Zhang, L.J. You, and Z.G. Zhao. 2018. "High Removal Performance of a Magnetic FPA90-Cl Anion Resin for Bromate and Coexisting Precursors: Kinetics, Thermodynamics, and Equilibrium Studies." *Environmental Science and Pollution Research* 25 (18): 18001–14. doi:10.1007/s11356-018-2029-8

Yan, H.M., X.J. Du, P. Li, S.L. Yu, and Y.L. Tang. 2015. "Adsorption of Bromate from Aqueous Solutions by Modified Granular Activated Carbon: Batch and Column Tests." *Ozone-Science & Engineering* 37 (4): 357–70. doi:10.1080/01919512.2014.1001020

Yang, J., Z. Dong, C. Jiang, C. Wang, and H. Liu. 2019a. "An Overview of Bromate Formation in Chemical Oxidation Processes: Occurrence, Mechanism, Influencing Factors, Risk Assessment, and Control Strategies." *Chemosphere* 237:124521. doi: 10.1016/j.chemosphere.2019.124521.

Yang, J., J. Li, W. Dong, J. Ma, Y Yang, J Li, Z. Yang, X. Zhang, J. Gu, W. Xie, et al. 2017. "Enhancement of Bromate Formation by pH Depression during Ozonation of bromide-containing Water in the Presence of

Hydroxylamine." *Water Research* 109:135–43. doi: 10.1016/j.watres.2016.11.037.

Yang, Y., Z. Zheng, W. Ji, M. Yang, Q. Ding, and X. Zhang. 2019b. "The Study of Bromate Adsorption onto Magnetic Ion Exchange Resin: Optimization Using Response Surface Methodology." *Surfaces and Interfaces* 17:100385. doi: 10.1016/j.surfin.2019.100385.

Yang, Q., Y. Zhong, X.M. Li, X. Li, K. Luo, X.Q. Wu, H.B. Chen, Y. Liu, and G.M. Zeng. 2015. "Adsorption-coupled Reduction of Bromate by Fe(II)-Al(III) Layered Double Hydroxide in fixed-bed Column: Experimental and Breakthrough Curves Analysis." *Journal of Industrial and Engineering Chemistry* 28:54–59. doi: 10.1016/j.jiec.2015.01.022.

Zhang, H., R. Deng, H.Y. Wang, Z.Y. Kong, D.Y. Dai, Z.H. Jing, W.S. Jiang, and Y. Hou. 2016. "Reduction of Bromate from Water by zero-valent Iron Immobilized on Functional Polypropylene Fiber." *Chemical Engineering Journal* 292:190–98. doi: 10.1016/j.cej.2016.02.010.